Fermilab-PUB-99/360-E
CDF/PUB/JET/PUBLIC/4760
December 10, 1999

A Measurement of the Differential Dijet Mass Cross Section in $p\bar{p}$ Collisions at $\sqrt{s} = 1.8$ TeV

T. Affolder,[21] H. Akimoto,[43] A. Akopian,[36] M. G. Albrow,[10] P. Amaral,[7] S. R. Amendolia,[32] D. Amidei,[24] K. Anikeev,[22] J. Antos,[1] G. Apollinari,[36] T. Arisawa,[43] T. Asakawa,[41] W. Ashmanskas,[7] M. Atac,[10] F. Azfar,[29] P. Azzi-Bacchetta,[30] N. Bacchetta,[30] M. W. Bailey,[26] S. Bailey,[14] P. de Barbaro,[35] A. Barbaro-Galtieri,[21] V. E. Barnes,[34] B. A. Barnett,[17] M. Barone,[12] G. Bauer,[22] F. Bedeschi,[32] S. Belforte,[40] G. Bellettini,[32] J. Bellinger,[44] D. Benjamin,[9] J. Bensinger,[4] A. Beretvas,[10] J. P. Berge,[10] J. Berryhill,[7] S. Bertolucci,[12] B. Bevensee,[31] A. Bhatti,[36] C. Bigongiari,[32] M. Binkley,[10] D. Bisello,[30] R. E. Blair,[2] C. Blocker,[4] K. Bloom,[24] B. Blumenfeld,[17] S. R. Blusk,[35] A. Bocci,[32] A. Bodek,[35] W. Bokhari,[31] G. Bolla,[34] Y. Bonushkin,[5] D. Bortoletto,[34] J. Boudreau,[33] A. Brandl,[26] S. van den Brink,[17] C. Bromberg,[25] M. Brozovic,[9] N. Bruner,[26] E. Buckley-Geer,[10] J. Budagov,[8] H. S. Budd,[35] K. Burkett,[14] G. Busetto,[30] A. Byon-Wagner,[10] K. L. Byrum,[2] M. Campbell,[24] A. Caner,[32] W. Carithers,[21] J. Carlson,[24] D. Carlsmith,[44] J. Cassada,[35] A. Castro,[30] D. Cauz,[40] A. Cerri,[32] A. W. Chan,[1] P. S. Chang,[1] P. T. Chang,[1] J. Chapman,[24] C. Chen,[31] Y. C. Chen,[1] M. -T. Cheng,[1] M. Chertok,[38] G. Chiarelli,[32] I. Chirikov-Zorin,[8] G. Chlachidze,[8] F. Chlebana,[10] L. Christofek,[16] M. L. Chu,[1] S. Cihangir,[10] C. I. Ciobanu,[27] A. G. Clark,[13] A. Connolly,[21] J. Conway,[37] J. Cooper,[10] M. Cordelli,[12] D. Costanzo,[32] J. Cranshaw,[39] D. Cronin-Hennessy,[9] R. Cropp,[23] R. Culbertson,[7] D. Dagenhart,[42] F. DeJongh,[10] S. Dell'Agnello,[12] M. Dell'Orso,[32] R. Demina,[10] L. Demortier,[36] M. Deninno,[3] P. F. Derwent,[10] T. Devlin,[37] J. R. Dittmann,[10] S. Donati,[32] J. Done,[38] T. Dorigo,[14] N. Eddy,[16] K. Einsweiler,[21] J. E. Elias,[10] E. Engels, Jr.,[33] W. Erdmann,[10] D. Errede,[16] S. Errede,[16] Q. Fan,[35] R. G. Feild,[45] C. Ferretti,[32] I. Fiori,[3] B. Flaugher,[10] G. W. Foster,[10] M. Franklin,[14] J. Freeman,[10] J. Friedman,[22] Y. Fukui,[20] S. Galeotti,[32] M. Gallinaro,[36] T. Gao,[31] M. Garcia-Sciveres,[21] A. F. Garfinkel,[34] P. Gatti,[30] C. Gay,[45] S. Geer,[10] D. W. Gerdes,[24] P. Giannetti,[32] P. Giromini,[12] V. Glagolev,[8] M. Gold,[26] J. Goldstein,[10] A. Gordon,[14] A. T. Goshaw,[9] Y. Gotra,[33] K. Goulianos,[36] H. Grassmann,[40] C. Green,[34] L. Groer,[37] C. Grosso-Pilcher,[7] M. Guenther,[34] G. Guillian,[24] J. Guimaraes da Costa,[24] R. S. Guo,[1] C. Haber,[21] E. Hafen,[22] S. R. Hahn,[10] C. Hall,[14] T. Handa,[15]

R. Handler,[44] W. Hao,[39] F. Happacher,[12] K. Hara,[41] A. D. Hardman,[34] R. M. Harris,[10] F. Hartmann,[18] K. Hatakeyama,[36] J. Hauser,[5] J. Heinrich,[31] A. Heiss,[18] M. Herndon,[17] B. Hinrichsen,[23] K. D. Hoffman,[34] C. Holck,[31] R. Hollebeek,[31] L. Holloway,[16] R. Hughes,[27] J. Huston,[25] J. Huth,[14] H. Ikeda,[41] J. Incandela,[10] G. Introzzi,[32] J. Iwai,[43] Y. Iwata,[15] E. James,[24] H. Jensen,[10] M. Jones,[31] U. Joshi,[10] H. Kambara,[13] T. Kamon,[38] T. Kaneko,[41] K. Karr,[42] H. Kasha,[45] Y. Kato,[28] T. A. Keaffaber,[34] K. Kelley,[22] M. Kelly,[24] R. D. Kennedy,[10] R. Kephart,[10] D. Khazins,[9] T. Kikuchi,[41] M. Kirk,[4] B. J. Kim,[19] H. S. Kim,[16] M. J. Kim,[19] S. H. Kim,[41] Y. K. Kim,[21] L. Kirsch,[4] S. Klimenko,[11] P. Koehn,[27] A. Köngeter,[18] K. Kondo,[43] J. Konigsberg,[11] K. Kordas,[23] A. Korn,[22] A. Korytov,[11] E. Kovacs,[2] J. Kroll,[31] M. Kruse,[35] S. E. Kuhlmann,[2] K. Kurino,[15] T. Kuwabara,[41] A. T. Laasanen,[34] N. Lai,[7] S. Lami,[36] S. Lammel,[10] J. I. Lamoureux,[4] M. Lancaster,[21] G. Latino,[32] T. LeCompte,[2] A. M. Lee IV,[9] S. Leone,[32] J. D. Lewis,[10] M. Lindgren,[5] T. M. Liss,[16] J. B. Liu,[35] Y. C. Liu,[1] N. Lockyer,[31] J. Loken,[29] M. Loreti,[30] D. Lucchesi,[30] P. Lukens,[10] S. Lusin,[44] L. Lyons,[29] J. Lys,[21] R. Madrak,[14] K. Maeshima,[10] P. Maksimovic,[14] L. Malferrari,[3] M. Mangano,[32] M. Mariotti,[30] G. Martignon,[30] A. Martin,[45] J. A. J. Matthews,[26] J. Mayer,[23] P. Mazzanti,[3] K. S. McFarland,[35] P. McIntyre,[38] E. McKigney,[31] M. Menguzzato,[30] A. Menzione,[32] C. Mesropian,[36] T. Miao,[10] R. Miller,[25] J. S. Miller,[24] H. Minato,[41] S. Miscetti,[12] M. Mishina,[20] G. Mitselmakher,[11] N. Moggi,[3] E. Moore,[26] R. Moore,[24] Y. Morita,[20] A. Mukherjee,[10] T. Muller,[18] A. Munar,[32] P. Murat,[32] S. Murgia,[25] M. Musy,[40] J. Nachtman,[5] S. Nahn,[45] H. Nakada,[41] T. Nakaya,[7] I. Nakano,[15] C. Nelson,[10] D. Neuberger,[18] C. Newman-Holmes,[10] C.-Y. P. Ngan,[22] P. Nicolaidi,[40] H. Niu,[4] L. Nodulman,[2] A. Nomerotski,[11] S. H. Oh,[9] T. Ohmoto,[15] T. Ohsugi,[15] R. Oishi,[41] T. Okusawa,[28] J. Olsen,[44] C. Pagliarone,[32] F. Palmonari,[32] R. Paoletti,[32] V. Papadimitriou,[39] S. P. Pappas,[45] D. Partos,[4] J. Patrick,[10] G. Pauletta,[40] M. Paulini,[21] C. Paus,[22] L. Pescara,[30] T. J. Phillips,[9] G. Piacentino,[32] K. T. Pitts,[10] R. Plunkett,[10] A. Pompos,[34] L. Pondrom,[44] G. Pope,[33] M. Popovic,[23] F. Prokoshin,[8] J. Proudfoot,[2] F. Ptohos,[12] G. Punzi,[32] K. Ragan,[23] A. Rakitine,[22] D. Reher,[21] A. Reichold,[29] W. Riegler,[14] A. Ribon,[30] F. Rimondi,[3] L. Ristori,[32] W. J. Robertson,[9] A. Robinson,[23] T. Rodrigo,[6] S. Rolli,[42] L. Rosenson,[22] R. Roser,[10] R. Rossin,[30] W. K. Sakumoto,[35] D. Saltzberg,[5] A. Sansoni,[12] L. Santi,[40] H. Sato,[41] P. Savard,[23] P. Schlabach,[10] E. E. Schmidt,[10] M. P. Schmidt,[45] M. Schmitt,[14] L. Scodellaro,[30] A. Scott,[5] A. Scribano,[32] S. Segler,[10] S. Seidel,[26] Y. Seiya,[41] A. Semenov,[8] F. Semeria,[3] T. Shah,[22] M. D. Shapiro,[21] P. F. Shepard,[33] T. Shibayama,[41] M. Shimojima,[41] M. Shochet,[7] J. Siegrist,[21] G. Signorelli,[32] A. Sill,[39] P. Sinervo,[23] P. Singh,[16] A. J. Slaughter,[45] K. Sliwa,[42] C. Smith,[17] F. D. Snider,[10] A. Solodsky,[36] J. Spalding,[10] T. Speer,[13] P. Sphicas,[22] F. Spinella,[32] M. Spiropulu,[14] L. Spiegel,[10] L. Stanco,[30] J. Steele,[44] A. Stefanini,[32] J. Strologas,[16] F. Strumia, [13] D. Stuart,[10] K. Sumorok,[22] T. Suzuki,[41] T. Takano,[28] R. Takashima,[15] K. Takikawa,[41] P. Tamburello,[9] M. Tanaka,[41] B. Tannenbaum,[5] W. Taylor,[23] M. Tecchio,[24] P. K. Teng,[1] K. Terashi,[41] S. Tether,[22] D. Theriot,[10] R. Thurman-Keup,[2] P. Tipton,[35] S. Tkaczyk,[10] K. Tollefson,[35] A. Tollestrup,[10] H. Toyoda,[28] W. Trischuk,[23] J. F. de Troconiz,[14] J. Tseng,[22] N. Turini,[32] F. Ukegawa,[41] J. Valls,[37] S. Vejcik III,[10]

G. Velev,[32] R. Vidal,[10] R. Vilar,[6] I. Volobouev,[21] D. Vucinic,[22] R. G. Wagner,[2] R. L. Wagner,[10] J. Wahl,[7] N. B. Wallace,[37] A. M. Walsh,[37] C. Wang,[9] C. H. Wang,[1] M. J. Wang,[1] T. Watanabe,[41] D. Waters,[29] T. Watts,[37] R. Webb,[38] H. Wenzel,[18] W. C. Wester III,[10] A. B. Wicklund,[2] E. Wicklund,[10] H. H. Williams,[31] P. Wilson,[10] B. L. Winer,[27] D. Winn,[24] S. Wolbers,[10] D. Wolinski,[24] J. Wolinski,[25] S. Wolinski,[24] S. Worm,[26] X. Wu,[13] J. Wyss,[32] A. Yagil,[10] W. Yao,[21] G. P. Yeh,[10] P. Yeh,[1] J. Yoh,[10] C. Yosef,[25] T. Yoshida,[28] I. Yu,[19] S. Yu,[31] A. Zanetti,[40] F. Zetti,[21] and S. Zucchelli[3]

(CDF Collaboration)

[1] *Institute of Physics, Academia Sinica, Taipei, Taiwan 11529, Republic of China*

[2] *Argonne National Laboratory, Argonne, Illinois 60439*

[3] *Istituto Nazionale di Fisica Nucleare, University of Bologna, I-40127 Bologna, Italy*

[4] *Brandeis University, Waltham, Massachusetts 02254*

[5] *University of California at Los Angeles, Los Angeles, California 90024*

[6] *Instituto de Fisica de Cantabria, University of Cantabria, 39005 Santander, Spain*

[7] *Enrico Fermi Institute, University of Chicago, Chicago, Illinois 60637*

[8] *Joint Institute for Nuclear Research, RU-141980 Dubna, Russia*

[9] *Duke University, Durham, North Carolina 27708*

[10] *Fermi National Accelerator Laboratory, Batavia, Illinois 60510*

[11] *University of Florida, Gainesville, Florida 32611*

[12] *Laboratori Nazionali di Frascati, Istituto Nazionale di Fisica Nucleare, I-00044 Frascati, Italy*

[13] *University of Geneva, CH-1211 Geneva 4, Switzerland*

[14] *Harvard University, Cambridge, Massachusetts 02138*

[15] *Hiroshima University, Higashi-Hiroshima 724, Japan*

[16] *University of Illinois, Urbana, Illinois 61801*

[17] *The Johns Hopkins University, Baltimore, Maryland 21218*

[18] *Institut für Experimentelle Kernphysik, Universität Karlsruhe, 76128 Karlsruhe, Germany*

[19] *Korean Hadron Collider Laboratory: Kyungpook National University, Taegu 702-701; Seoul National University, Seoul 151-742; and SungKyunKwan University, Suwon 440-746; Korea*

[20] *High Energy Accelerator Research Organization (KEK), Tsukuba, Ibaraki 305, Japan*

[21] *Ernest Orlando Lawrence Berkeley National Laboratory, Berkeley, California 94720*

[22] *Massachusetts Institute of Technology, Cambridge, Massachusetts 02139*

[23] *Institute of Particle Physics: McGill University, Montreal H3A 2T8; and University of Toronto, Toronto M5S 1A7; Canada*

[24] *University of Michigan, Ann Arbor, Michigan 48109*

[25] *Michigan State University, East Lansing, Michigan 48824*

[26] *University of New Mexico, Albuquerque, New Mexico 87131*

[27] *The Ohio State University, Columbus, Ohio 43210*

[28] *Osaka City University, Osaka 588, Japan*

[29] *University of Oxford, Oxford OX1 3RH, United Kingdom*

[30] *Universita di Padova, Istituto Nazionale di Fisica Nucleare, Sezione di Padova, I-35131 Padova, Italy*

[31] *University of Pennsylvania, Philadelphia, Pennsylvania 19104*
[32] *Istituto Nazionale di Fisica Nucleare, University and Scuola Normale Superiore of Pisa, I-56100 Pisa, Italy*
[33] *University of Pittsburgh, Pittsburgh, Pennsylvania 15260*
[34] *Purdue University, West Lafayette, Indiana 47907*
[35] *University of Rochester, Rochester, New York 14627*
[36] *Rockefeller University, New York, New York 10021*
[37] *Rutgers University, Piscataway, New Jersey 08855*
[38] *Texas A&M University, College Station, Texas 77843*
[39] *Texas Tech University, Lubbock, Texas 79409*
[40] *Istituto Nazionale di Fisica Nucleare, University of Trieste/ Udine, Italy*
[41] *University of Tsukuba, Tsukuba, Ibaraki 305, Japan*
[42] *Tufts University, Medford, Massachusetts 02155*
[43] *Waseda University, Tokyo 169, Japan*
[44] *University of Wisconsin, Madison, Wisconsin 53706*
[45] *Yale University, New Haven, Connecticut 06520*

Abstract

We present a measurement of the cross section for production of two or more jets as a function of dijet mass, based on an integrated luminosity of 86 pb^{-1} collected with the Collider Detector at Fermilab. Our dijet mass spectrum is described within errors by next-to-leading order QCD predictions using CTEQ4HJ parton distributions, and is in good agreement with a similar measurement from the DØ experiment.

PACS numbers: 13.85.Rm, 12.38.Qk,

Hard collisions between protons and antiprotons predominantly produce dijet events, which are events containing at least two high energy jets. A measurement of the dijet mass differential cross section provides a fundamental test of Quantum Chromodynamics (QCD) and a constraint on the parton distributions of the proton. We previously reported measurements of the inclusive jet transverse energy (E_T) spectrum [1] and the cross section for events with large total E_T [2]. Both measurements indicated an excess of events at high E_T compared to the predictions of QCD. This letter presents our most recent measurement of the dijet mass spectrum [3] and compares it with the predictions of next-to-leading order QCD and the measurement of DØ [4]. This measurement, with an integrated luminosity of 86 pb^{-1}, is significantly more sensitive to events at high dijet mass than our previous measurements of the dijet mass spectrum [5] with integrated luminosities of 4.2 pb^{-1} and 26 nb^{-1}. We recently used this data sample combined with 20 pb^{-1} of older data to measure dijet angular distributions [6] and to search the dijet mass spectrum for new particles decaying to dijets [7].

A detailed description of the Collider Detector at Fermilab (CDF) can be found elsewhere [8]. We use a coordinate system with the z axis along the proton beam, transverse coordinate perpendicular to the beam, azimuthal angle ϕ, polar angle θ, and pseudorapidity $\eta = -\ln\tan(\theta/2)$. Jets are reconstructed as localized energy depositions in the CDF calorimeters, which are arranged in a projective tower geometry. The jet energy, E, is defined as the scalar sum of the calorimeter tower energies inside a cone of radius $R = \sqrt{(\Delta\eta)^2 + (\Delta\phi)^2} = 0.7$, centered on the jet direction. Jets that share towers are combined if the total E_T of the shared towers is greater than 75% of the E_T of either jet; otherwise the towers are assigned to the nearest jet. The jet momentum, $\vec{P}$, is the vector sum: $\vec{P} = \sum E_i \hat{u}_i$, with $\hat{u}_i$ being the unit vector pointing from the interaction point to the energy deposition E_i inside the cone. The quantities E and $\vec{P}$ are corrected for calorimeter non-linearities, energy lost in uninstrumented regions of the detector, and energy gained from the underlying event and additional $p\bar{p}$ interactions. We do not correct for energy lost outside the clustering cone, since a similar loss is present in the $O(\alpha_s^3)$ QCD calculation in which an extra gluon can be radiated outside the jet clustering cone. The jet energy corrections increase the measured jet energies on average by 20% (16%) for 100 GeV (400 GeV) jets. Full details of jet reconstruction and jet energy corrections at CDF can be found elsewhere [9].

We define the dijet system as the two jets with the highest transverse momentum in an event (leading jets) and define the dijet mass as $M = \sqrt{(E_1 + E_2)^2 - (\vec{P}_1 + \vec{P}_2)^2}$. Our data sample was obtained using four triggers that required at least one jet with uncorrected cluster transverse energies of 20, 50, 70 and 100 GeV, respectively. After correcting the jet energies these trigger samples were used to measure the dijet mass spectrum above 180, 217, 292, and 388 GeV/c^2, respectively, where the trigger efficiencies were greater than 97%. The four data samples corresponded to integrated luminosities of 0.091, 2.2, 11, and 86 pb^{-1} respectively. We selected events with two or more jets and required that the two leading jets have pseudorapidities of $|\eta_1| < 2$

and $|\eta_2| < 2$ and satisfy $|\cos\theta^*| = |\tanh[(\eta_1 - \eta_2)/2]| < 2/3$, where θ^* is the scattering angle in the dijet center-of-mass frame. The $\cos\theta^*$ requirement ensures full acceptance as a function of the dijet mass. The z position of the event vertex was required to be within 60 cm of the center of the detector; this cut removed 6% of the events. Backgrounds from cosmic rays, beam halo, and detector noise were removed by requiring $\not\!\!E_T/\sqrt{\sum E_T} < 6$ GeV$^{1/2}$ and $\sum E < 2$ TeV, where $\not\!\!E_T$ is the missing transverse energy [10], $\sum E_T$ is the total transverse energy (scalar sum), and $\sum E$ is the total energy in the event. These cuts selected 60,998 events.

The dijet mass resolution was determined using the PYTHIA [11] Monte Carlo program and a CDF detector simulation. The true jet is defined from the true E_T of particles emanating from the hard scattering, using the same jet algorithm as described above, but applied to towers of true E_T. The true E_T of a tower is the E_T of the generated particles that enter the tower. The simulated jet uses the E_T of simulated calorimeter towers and the jet energy corrections for the CDF detector simulation. The E_T of the simulated jets is corrected to equal the E_T of the corresponding true jet on average. The dijet mass resolution function, $\rho(M, m)$, is then defined as the distribution of simulated dijet masses, M, for each value of true dijet mass, m. The dijet mass resolution was determined for six values of m between 50 and 1000 GeV/c^2 and then a single smooth parameterization was used to interpolate between these values. The dijet mass resolution is approximately 10% for dijet masses above 150 GeV/c^2.

The steeply falling dijet mass spectrum is distorted by the dijet mass resolution.

We correct for this distortion with an unsmearing procedure. Define the smeared spectrum, $S(M)$, as the convolution of the true spectrum, $T(m)$, and the dijet mass resolution: $S(M) = \int T(m)\rho(M,m)dm$. We parameterize the true dijet mass spectrum with $T(m) = A(1 - m/\sqrt{s} + Cm^2/s)^N/m^P$ where $\sqrt{s} = 1800$ GeV. We then fit the smeared spectrum to our data to find the value of the four parameters $A = 6.67 \times 10^{17}$pb/(GeV/c^2), $C = 2.95$, $N = -6.98$, and $P = 6.70$. The fit has a χ^2 of 20.5 for 14 degrees of freedom. The unsmearing correction factors, K_i, are then defined as the ratio of the smeared to true spectrum, $K_i = \int_i S(M)dM / \int_i T(m)dm$, where the integration is over mass bin i. The value of K_i smoothly decreases from 1.07 at $M = 188$ GeV/c^2, to 1.03 at $M = 540$ GeV/c^2, and then smoothly increases to 1.12 at $M = 968$ GeV/c^2. The corrected cross section as a function of dijet mass is given by

$$d\sigma/dM = n_i/(K_i\ \mathcal{L}\ \epsilon_i\ \Delta M), \tag{1}$$

where for each mass bin i, n_i is the number of events, $\mathcal{L}$ is the integrated luminosity, ϵ_i is the efficiency of the trigger and z-vertex selections, and ΔM is the width of the mass bin.

In Table I we list 12 independent sources of systematic uncertainty in the dijet mass cross section. They are the uncertainties in calorimeter calibration (cal), jet fragmentation (frag), underlying event (uevt), calorimeter stability over time (stab), relative jet energy scale as a function of pseudorapidity [6] (rel), detector simulation (sim), the unsmearing procedure (unsm), the tails of the resolution function (tails), absolute luminosity [12] of the jet 100 trigger (lum), and the relative luminosities of the jet 20, 50 and 70 triggers (J20, J50, and J70). The first four systematic uncertainties [1] are equivalent to a combined uncertainty in the determination of the dijet mass variable which decreases from 2.7% at $M = 188$ GeV/c^2 to 2.3% at $M = 968$ GeV/c^2. The uncertainty in detector simulation results from a 0.5% uncertainty in the equality of the true dijet mass and the simulated dijet mass after all jet corrections are applied, independent from the first four systematic uncertainties mentioned above. To check that our unsmearing procedure is internally consistent, we applied the unsmearing procedure to a simulated dijet mass spectrum. The resulting K_i were in agreement with the ratios of the simulated spectrum to true spectrum for each mass bin. Due to limited Monte Carlo statistics, the systematic uncertainty on the consistency of the unsmearing procedure was 4%. The uncertainty in the dijet mass resolution due to non-Gaussian tails was estimated by repeating the unsmearing procedure with a Gaussian resolution. The systematic uncertainties on the luminosity for the jet 20, 50 and 70 triggers came from the statistical uncertainty in matching the cross section of each trigger with the next higher threshold trigger (jet 70 was required to match jet 100 in the first bin of the jet 100 sample, jet 50 was required to match jet 70, etc.) Each of the independent systematic uncertainties in Table I are completely correlated as a function of dijet mass.

In Table II we present the fully corrected inclusive dijet mass spectrum for $p\bar{p} \rightarrow$ 2 jets + X, where X can be anything, including additional jets. We tabulate the differential cross section versus the mean dijet mass in bins of width approximately equal to the dijet mass resolution. Figure 1 shows the fractional difference between our data and $O(\alpha_s^3)$ QCD predictions from the parton level event generator JETRAD [13]. Here the renormalization scale is $\mu = 0.5E_T^{max}$, where E_T^{max} is the maximum jet E_T in the generated event. In the JETRAD calculation, two partons are combined if they are within $R_{sep} = 1.3R$, which corresponds to the separation of jets in the data. Predictions are shown for various choices of parton distribution functions: CTEQ4M [14] and MRST [15] are standard sets and CTEQ4HJ [14] adjusts the gluon distribution to give a better fit to the CDF inclusive jet E_T spectrum at high E_T. Figure 1 shows that the CTEQ4HJ prediction models the shape and normalization of our dijet data better than CTEQ4M. The CTEQ4M prediction changes by less than 5% when the renormalization scale is changed to $\mu = E_T^{max}$, but it decreases between 7% and 17% for $\mu = 2E_T^{max}$, and it decreases between 25% and 30% for $\mu = 0.25E_T^{max}$. In Fig. 2 we compare the fractional difference between our data and QCD with that of the D∅ experiment. The D∅ measurement [4] and the JETRAD prediction obtained by D∅ required that each jet be in region $|\eta| < 1.0$. Figure 2 shows that our data and the D∅ data are in good agreement.

The covariance matrix for the dijet mass differential cross section is defined as $V_{ij} = \delta_{ij}\sigma_i^2(stat) + \Sigma_{k=1}^{12}\sigma_i(sys_k)\sigma_j(sys_k)$. Here $\delta_{ij} = 1(0)$ for $i = j (i \neq j)$, $\sigma_i(stat)$ is the statistical uncertainty in mass bin i, and the sum is over each of the 12 systematic uncertainties $\sigma_i(sys_k)$ listed in Table I. Since the theory always predicts a smaller cross section than the data, the positive percent systematic uncertainty given in Table I was multiplied by the theoretical cross section to determine the $\sigma_i(sys_k)$. From the inverse of the covariance matrix, $(V^{-1})_{ij}$, and the difference between the data and the theory in each bin, Δ_i, we perform a χ^2 comparison between the data and the theory. Table III presents values for $\chi^2 = \Sigma_{i,j}\Delta_i(V^{-1})_{ij}\Delta_j$ and the corresponding probability for a standard χ^2 distribution with 18 degrees of freedom (14 degrees of freedom for the row labeled Fit). Our data is in agreement within errors with the QCD prediction using CTEQ4HJ parton distributions, which has an enhanced gluon distribution at high E_T. Our data excludes CTEQ4M parton distributions, which have a standard gluon distribution. The χ^2 comparison shows that our data cannot exclude with high confidence QCD predictions using MRST parton distributions, even though the normalization of that prediction is well beneath that of our data. This is because of the presence of correlated systematic uncertainties that are large compared with the statistical uncertainties. Such correlated uncertainties can accommodate certain significant deviations in both normalization and shape between the data and the theory with a relatively small penalty in χ^2. Any theoretical prediction whose deviation from the data matches the shape of a correlated uncertainty will give a reasonable χ^2 provided that the normalization difference between the data and the prediction is no more than a few standard deviations.

In conclusion, we have measured the cross section for production of two or more jets in the kinematic region $|\eta| < 2$ and $|\cos\theta^*| < 2/3$ as a function of dijet invariant mass. The data at the highest values of dijet mass are above the QCD predictions using standard parton distributions, similar to the excess at high E_T observed in previous measurements of the inclusive jet E_T spectrum [1] and the total E_T spectrum [2]. The CDF data are described within errors by next-to-leading order QCD predictions using CTEQ4HJ parton distributions, and are in good agreement with a similar measurement from the DØ experiment.

We thank the Fermilab staff and the technical staffs of the participating institutions for their vital contributions. This work was supported by the U.S. Department of Energy and National Science Foundation; the Italian Istituto Nazionale di Fisica Nucleare; the Ministry of Education, Science and Culture of Japan; the Natural Sciences and Engineering Research Council of Canada; the National Science Council of the Republic of China; the Swiss National Science Foundation; the A. P. Sloan Foundation; the Bundesministerium fuer Bildung und Forschung, Germany; and the Korea Science and Engineering Foundation.

References

[1] F. Abe *et al.*, Phys. Rev. Lett. **77**, 438 (1996).

[2] F. Abe *et al.*, Phys. Rev. Lett. **80**, 3461 (1998).

[3] B. Hinrichsen, Ph.D. thesis, University of Toronto, 1999 (unpublished).

[4] B. Abbott *et al.*, Phys. Rev. Lett. **82**, 2457 (1999).

[5] F. Abe *et al.*, Phys. Rev. **D48**, 998 (1993) and Phys. Rev. **D41**, 1722 (1990).

[6] F. Abe *et al.*, Phys. Rev. Lett. **77**, 5336 (1996).

[7] F. Abe *et al.*, Phys. Rev. **D55**, R5263 (1997).

[8] F. Abe *et al.*, Nucl. Instrum. and Methods **A271**, 387 (1988).

[9] F. Abe *et al.*, Phys. Rev. **D45**, 1448 (1992).

[10] F. Abe *et al.*, Phys. Rev. Lett. **66**, 2951 (1991).

[11] T. Sjöstrand, Comput. Phys. Commun. **82**, 74 (1994).

[12] D. Cronin-Hennessy *et al.*, Fermilab-PUB-99/162-E, to be published in Nucl. Instrum. and Methods.

[13] W.T. Giele, E.W.N. Glover, and D.A. Kosower, Nucl. Phys. **B403**, 633 (1993). We used JETRAD version 2.0.

[14] H. L. Lai *et al.*, Phys. Rev. **D55**, 1280 (1997).

[15] A.D. Martin, R.G. Roberts, W.J. Stirling, and R.S. Thorne, Eur. Phys. J. C**4**, 463 (1998).

Table I: Systematic uncertainties on the cross section (see text).

Mass	Systematic Uncertainty on Cross Section in %											
(GeV/c^2)	cal	frag	uevt	stab	rel	sim	unsm	tails	lum	J20	J50	J70
188	$^{+12}_{-8}$	$^{+8}_{-7}$	$^{+8}_{-7}$	$^{+7}_{-6}$	5	2	4	2	4	4	2	2
207	$^{+12}_{-8}$	$^{+8}_{-7}$	7	$^{+7}_{-6}$	5	2	4	2	4	4	2	2
228	$^{+12}_{-8}$	$^{+8}_{-7}$	6	$^{+7}_{-6}$	$^{+6}_{-5}$	3	4	3	4	–	2	2
252	$^{+12}_{-8}$	$^{+8}_{-7}$	6	$^{+7}_{-6}$	6	3	4	3	4	–	2	2
277	$^{+12}_{-8}$	$^{+8}_{-7}$	5	$^{+7}_{-6}$	6	3	4	4	4	–	2	2
305	$^{+12}_{-8}$	8	5	7	6	4	4	4	4	–	–	2
335	$^{+12}_{-8}$	$^{+8}_{-7}$	$^{+5}_{-4}$	$^{+7}_{-6}$	6	4	4	5	4	–	–	2
368	$^{+13}_{-8}$	$^{+8}_{-8}$	$^{+5}_{-4}$	7	$^{+7}_{-6}$	5	4	5	4	–	–	2
405	$^{+13}_{-9}$	8	4	$^{+8}_{-7}$	$^{+7}_{-6}$	5	4	5	4	–	–	–
446	$^{+14}_{-9}$	$^{+9}_{-8}$	4	$^{+8}_{-7}$	7	5	4	6	4	–	–	–
491	$^{+14}_{-9}$	$^{+9}_{-8}$	4	8	7	6	4	6	4	–	–	–
539	$^{+15}_{-10}$	$^{+10}_{-9}$	$^{+4}_{-3}$	$^{+9}_{-8}$	$^{+8}_{-7}$	6	4	7	4	–	–	–
592	$^{+16}_{-11}$	$^{+10}_{-9}$	3	9	$^{+8}_{-7}$	6	4	7	4	–	–	–
652	$^{+17}_{-11}$	$^{+11}_{-10}$	3	$^{+10}_{-9}$	$^{+8}_{-7}$	7	4	7	4	–	–	–
716	$^{+19}_{-12}$	$^{+12}_{-11}$	3	$^{+11}_{-10}$	8	7	4	8	4	–	–	–
784	$^{+20}_{-13}$	$^{+13}_{-11}$	3	$^{+12}_{-10}$	$^{+9}_{-8}$	7	4	8	4	–	–	–
865	$^{+22}_{-14}$	$^{+14}_{-12}$	3	$^{+13}_{-11}$	$^{+9}_{-8}$	8	4	9	4	–	–	–
968	$^{+24}_{-15}$	$^{+15}_{-13}$	3	$^{+14}_{-12}$	$^{+9}_{-8}$	8	4	9	4	–	–	–

Table II: For each bin we list the average dijet mass, the differential cross section, and the statistical and total systematic uncertainty on the cross section.

bin edge (GeV/c^2)	average M (GeV/c^2)	$d\sigma/dM$ (pb/GeV/c^2)	statistical uncertainty	systematic uncertainty
180	188	6.07×10^{2}	3.2 %	$^{+20}_{-17}$ %
198	207	3.42×10^{2}	4.1 %	$^{+19}_{-17}$ %
217	228	1.81×10^{2}	1.0 %	$^{+19}_{-16}$ %
241	252	9.81×10^{1}	1.4 %	$^{+19}_{-16}$ %
265	277	4.98×10^{1}	1.8 %	$^{+19}_{-17}$ %
292	305	2.78×10^{1}	1.1 %	$^{+19}_{-17}$ %
321	335	1.43×10^{1}	1.4 %	$^{+20}_{-17}$ %
353	368	7.41×10^{0}	1.9 %	$^{+20}_{-18}$ %
388	405	3.83×10^{0}	0.9 %	$^{+21}_{-18}$ %
427	446	1.89×10^{0}	1.2 %	$^{+21}_{-19}$ %
470	491	9.07×10^{-1}	1.7 %	$^{+22}_{-19}$ %
517	539	4.50×10^{-1}	2.3 %	$^{+23}_{-20}$ %
568	592	1.90×10^{-1}	3.3 %	$^{+25}_{-21}$ %
625	652	7.42×10^{-2}	5.1 %	$^{+26}_{-22}$ %
688	716	2.92×10^{-2}	7.7 %	$^{+28}_{-23}$ %
756	784	1.18×10^{-2}	11 %	$^{+30}_{-25}$ %
832	865	3.57×10^{-3}	20 %	$^{+32}_{-26}$ %
915	968	9.03×10^{-4}	33 %	$^{+34}_{-28}$ %

Table III: χ^2 and corresponding probability for theoretical predictions for the dijet mass spectrum with various choices of parton distribution functions and renormalization scales $\mu = DE_T^{max}$. The row labeled Fit is the parameterization used in the unsmearing (see text).

PDF	D	χ^2	Probability
CTEQ4M	0.25	66.0	2.2×10^{-7}
	0.5	48.9	1.1×10^{-4}
	1.0	48.1	1.5×10^{-4}
	2.0	52.5	1.7×10^{-5}
CTEQ4HJ	0.5	29.8	4.0×10^{-2}
	1.0	26.1	9.8×10^{-2}
CTEQ3M	0.5	45.7	3.3×10^{-4}
	1.0	55.2	1.2×10^{-5}
MRST	0.5	38.7	3.2×10^{-3}
	1.0	33.5	1.5×10^{-2}
MRST(g$\uparrow$)	0.5	36.1	6.9×10^{-3}
MRST(g$\downarrow$)	0.5	38.3	3.5×10^{-3}
Fit	–	20.5	1.2×10^{-1}

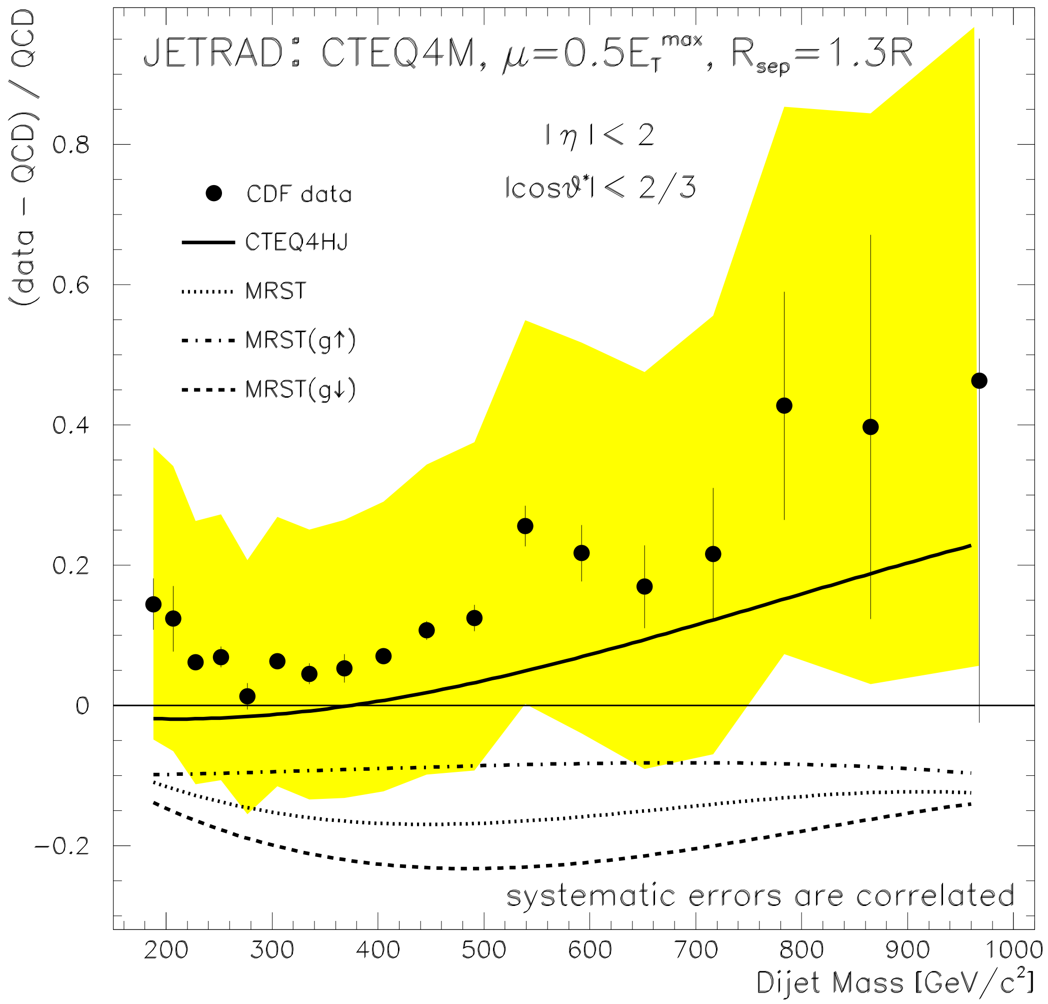

Figure 1: The fractional difference between the measured differential cross section and the QCD prediction (points) as a function of dijet mass. The band is the systematic uncertainty. The curves are the fractional difference between other QCD predictions, for various choices of parton distributions, and our default QCD prediction using CTEQ4M.

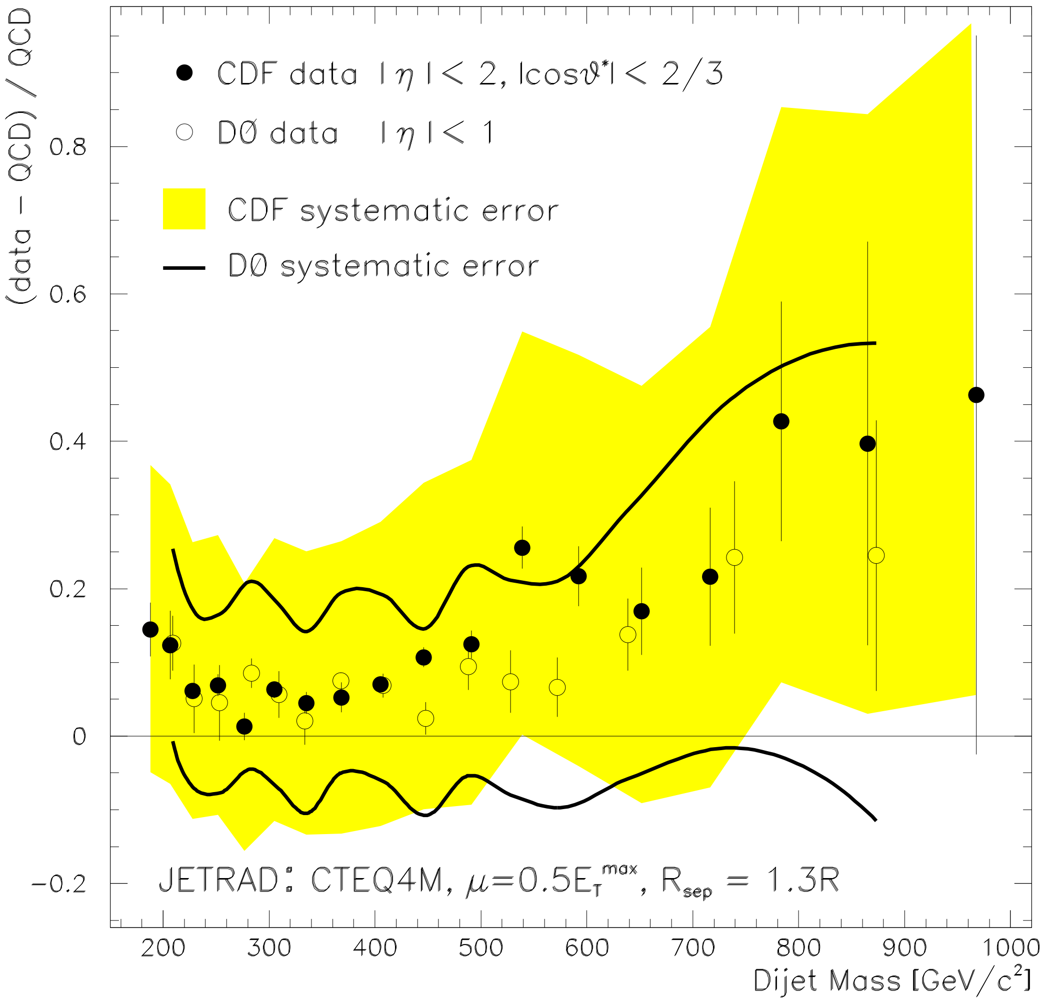

Figure 2: The difference between CDF data and QCD (solid points as shown in Fig. 1) compared to the difference between DØ data [4] and QCD (open points). The solid curves are the DØ systematic uncertainty.